Challenging the impact of consortium diversity on bioaugmentation efficiency and native bacterial community structure in a freshly PAH-contaminated soil

E.E. Nieto[a] *, S. Festa [a]*, D. Colman[a] I. S. Morelli [a,b], B. M. Coppotelli [a]

a) Centro de Investigación y Desarrollo en Fermentaciones Industriales, CINDEFI (UNLP; CCT-La Plata, CONICET), La Plata, Argentina

b) Comisión de Investigaciones Científicas de la Provincia de Buenos Aires, La Plata, Argentina

*=Authors contributed equally to this manuscript

Correspondence: Bibiana M. Coppotelli

CINDEFI, Street 50 N°227, 1900 La Plata, Argentina

Tel/Fax: +54 221 4833794

E-mail: bibicoppotelli@gmail.com

ORCID: 0000-0003-3439-5170

Keywords: bacterial consortia, allochthonous bioaugmentation, ANCOM-BC, substrate availability, inoculum establishment

Abstract

Polycyclic aromatic hydrocarbons (PAHs) are priority pollutants. We studied the effect of bioaugmentation with three allochthonous bacterial consortia with increasing diversity, SC AMBk, SC1 and SC4, in the structure and functionality of an acutely PAH-contaminated soil microbiome. The PAH supplementation increased the resource availability and the inocula were able to: efficiently degrade the PAHs supplemented after 15 days of incubation, become temporary established, and modify the number of total interactions with soil residents. *Sphingobium* and *Burkholderia,* both member of inoculants, were the major contributors to KO linked to degradation and to differentially abundant

genera in inoculated microcosms, indicating their competitiveness in the soil. Bioaugmentation efficiency relayed on them, while further degradation, could be carried out by native microorganism. This is the one of the first works which applied three inocula, designed from naturally occurring bacteria and study their effect on the soil native community through the ANCOM-BC. We revealed that when a resource that can be use by the inoculant is added to the soil, it is not necessary a high-diversity inoculant to interact with native community and establish itself. This result has implications in the design of microbiome engineering for bioremediation processes

1. Introduction

Polycyclic aromatic hydrocarbons (PAHs), produced mainly by anthropogenic sources, are priority organic pollutants, according to the US Environmental Protection Agency, affecting the health of humans and other organisms (Ravindra et al., 2008; García-Sánchez et al., 2018; Patel et al., 2020). The metabolism of some PAHs generates intermediates (e.g., diol epoxides, quinones, hydroxyalkyl derivatives), which form covalent adducts with nucleic acid and lead to genotoxic effects (Abdel-Shafy and Mansour, 2016). Due to their hydrophobicity, these contaminants are easily adsorbed into soil particles and, therefore, soils function as a reservoir of PAHs (Kuppusamy et al., 2017).

Bioremediation is a cost-effective and ecofriendly technology to reduce the concentration of pollutants from environmental matrices (Patel et al., 2020). In order to do so, it is key to apply in situ microbiome engineering approach, which aims to control and design community-level properties through (Lawson, 2021) the manipulation of indigenous microbes or the introduction of new members (Albright et al., 2022). As microbiome engineering through bioaugmentation, seeks to generate microbiomes with new functionalities (e.g. degradation of a target pollutant), it has been proposed as a powerful tool to improve environmental bioremediation of PAH (Wanapaisan et al., 2018; Laothamteep et al., 2021).

An effective strategy for bioremediation of acutely contaminated soils is the inoculation of allochthonous PAH-degrading microorganisms (Nwankwegu et al., 2022). The use of microbial

consortia as inocula in bioremediation processes became relevant in recent times, since the interactions between their members can optimize the degradation processes (Massot et al., 2022). Positive interactions favor consortia stability and robustness, which can be correlated with consortia diversity, and increase the probability of inoculum establishment (Stenuit and Agathos, 2015; Che and Men, 2019; McCarty and Ledesma-Amaro, 2019; Ziesack et al., 2019). Also, pre-existing interactions in consortia can be exploited by creating highly specialized microbial units where organisms fulfill certain niches (Albright et al., 2022).

A crucial aspect in bioremediation processes is the understanding of microbial diversity, community structure, interactions, and metabolic activities (Muangchinda et al., 2018). Soil microbes co-exist in complex networks with multiple interactions that influence the functional stability of soil ecological system(Fath et al., 2007; Wang et al., 2018; Shi et al., 2020; Tu et al., 2020). A novel perspective posits that microbial communities are organized into metabolically cohesive units where consortia with positive feedback loops use resources in a stable manner and minimize competition through resource specialization and exclusion of generalists (Pascual-García et al., 2020). Synthetic consortium has been described as forming stable microbiomes with previously established community members, as long as key players can compete with resident microorganisms (Lawson, 2021).

Bioaugmentation strategies could fail due to the lack of microorganisms performing critical functions (Iwabuchi et al., 2002), or because consortia selected under laboratory conditions are outcompeted by the native community in the field (Palkova, 2004; Steensels et al., 2019). Monitoring inoculants is needed to determine whether the desired functional changes were achieved as a consequence of the establishment or modification of desired functions in the community (Cornell et al., 2021; Albright et al., 2022). Furthermore, the introduction of new species during bioaugmentation can have a relevant impact on the native community, even when the abundance of the inoculant decreases (Mallon et al., 2018; Mawarda et al., 2020). Therefore, soil microbiome engineering efforts should consider the assessment of establishment of the inoculants and the footprint left in the native community after the

bioaugmentation process and not only inoculant characteristics (Kaminsky et al., 2019; Manfredini et al., 2021).

In previous works, three PAH-degrading synthetic consortia from naturally occurring bacteria were designed: SC AMBk, SC1 and SC4 consortia, which differed in number and composition of bacterial species (Macchi et al., 2021; Nieto et al., 2023). Their degradation potential was evaluated encompassing the individual strain roles, the interaction among strains and time-driven changes in gene expression and metaproteomic patterns during PAH removal. These consortia increased, due to synergistic interactions, the degradation efficiency of PAHs in liquid medium in relation to axenic cultures, positing them as good candidates for application in bioaugmentation processes (Macchi et al., 2021; Nieto et al., 2023).

This work evaluates the effects of the three allochthonous bacterial inocula, SC AMBk, SC1 and SC4, in the structure and functionality of a native microbial community of an acutely contaminated soil and monitors the constituent strains in soil during the bioaugmentation process. We hypothesized that when using a more diverse inoculant in bioaugmentation strategies, an improvement in pollutant degradation activity will be observed due to different microbiome assemblies. This was carried out as part of a continued effort to develop and refine an *in situ* microbiome engineering scheme to remediate PAH-contaminated sites. The novelty of this work is the use of three inocula designed from naturally occurring bacteria for the bioaugmentation experiments, the monitoring of the constituent strains of the inoculated consortia and the comparison of the effect on the soil native community through the ANCOM-BC (Analysis of Compositions of Microbiomes with Bias Correction).

2 Materials and methods

2.1 Soil Samples

Non-contaminated soil (SP) samples were collected from an urban park near La Plata city, Argentina (34°51'24.6"S;58°06'54.2"W). Physicochemical properties were determined in the Laboratory of Soil Science at the National University of La Plata. SP soil was a clay loam soil with a pH of 5.8-5.9, 3.60%

104 organic carbon, 6.21% soil organic matter, 0.296% total nitrogen, 4.2 $mg.kg^{-1}$ available phosphorus and
105 no hydrocarbons were detected.

106 **2.2 Defined Consortia preparation**

107 SC AMBk, SC1 and SC4 were constructed with different combinations of the strains *Sphingobium* sp
108 AM*, Burkholderia* sp Bk, *Pseudomonas* sp Bc-h and T, *Inquilinus limosus* Inq, and *Klebsiella aerogenes*
109 B, all belonging to an enrichment culture CON (Festa et al., 2013; Macchi et al., 2021). Each strain was
110 grown independently in R3 broth at 28°C and 150 rpm overnight, then the cells were harvested by
111 centrifugation at 6000 rpm and washed twice with sterile NaCl 0.85% (w/v). Cell number of each
112 suspension was determined measuring O.D at 580 nm. SC AMBk was composed of the strains AM and
113 Bk in a 65:35 ratio, being AM the major strain; SC1 was composed of the strains AM, T, Bc-h, B and Inq;
114 and SC4 of AM, Bk, T, Bc-h, B and Inq. Both SC1 and SC4 were built with equal proportions of each
115 strain.

116 **2.3 Microcosms set up.**

117 Microcosms of SP soil were constructed with 150 g of sieved soil (2 mm mesh) in 350 ml glass
118 containers. SP soil was contaminated with a mix solution containing 150 mg.kg dry $soil^{-1}$ of fluorene
119 (FLU), 600 mg.kg dry $soil^{-1}$ phenanthrene (PHE), 100 mg.kg dry $soil^{-1}$ anthracene (ANT), and 150 mg.kg
120 dry $soil^{-1}$ pyrene (PYR) to a final concentration of 1000 mg.kg dry $soil^{-1}$ of PAH. The spiking solution was
121 added one day before inoculation. Five treatments were carried out in triplicate: 1) microcosm without
122 contamination or inoculation (non-contaminated or control); 2) microcosm contaminated with the
123 spiking solution but without inoculation (SP+PAH); and the three inoculated treatments were
124 inoculated with $5*10^7$ $CFU.ml^{-1}$ of 3) SC AMBk; 4) SC1; 5) SC4.

125 The final moisture was adjusted to 20% humidity. All microcosms were incubated during 58 days at
126 24±°C and were mixed weekly for aeration.

127 **2.4 PAH quantification**

128 PAH concentration was determined on 5 g of soil sampled from each microcosm at 0, 15, 30, and 58
129 days of incubation. Samples were lyophilized (L-3, REFICOR) and three consecutive extractions were

130 carried out, using 15 ml of hexane:acetone 1:1 (v/v). The hydrocarbons were extracted in an ultrasonic
131 bath (Testlab Ul-trasonic TB10TA) at 40 kHz, 400 W for 30 min. The mixture was centrifuged at 3000
132 rpm for 10 min and the supernatants were collected in brown glass flasks and evaporated. Then,
133 samples were resuspended in 2 ml of hexane: acetone and filtered (0.45-µm nylon membrane). 5 µl of
134 each sample was injected into a Perkin Elmer Clarus 500 GC-FID. The oven temperature was
135 programmed from 100 °C (initial time 2 min) to 170°C (40 °C.min^{-1}) in the first step, 190°C (10°C.min^{-1})
136 in the second step, and to 250°C (40°C.min^{-1}), following and extension phase of 2 min. The retention
137 times of the different PAH were determined with standard solution and quantified using calibration
138 curves through serial dilutions.

139 **2.5 DNA extraction and Real time PCR**

140 Total DNA was extracted from 1 g of soil from each triplicate microcosm at 0, 15, 30 and 58 days using
141 the e E.Z.N.A. Soil DNA Kit (Omega Bio-Tek, Inc., USA) following the manufacturer's instructions, and
142 DNA was quantified with NanoDrop 2000 (Thermo Fisher).

143 Copy number of PAH-degradation related genes: PAHs ring-hydroxylating α subunit-dioxygenase of
144 Gram-negative (GN PAH-RHDα) (Cebron et al., 2008) and catechol 2,3 dioxygenase (C230) (Sei et al
145 1999), and eubacterial 16S rRNA gene (Harms et al 2003) were quantified by qPCR in a Rotor-Gene Q
146 2plex (QIAGEN). qPCR reactions were performed in 10 µl final volume, contained 2 µl of template DNA,
147 5 µl 2x SsoAdvancedTM Universal SYBR Green Supermix (Bio Rad), 1 µl of each primer (0.4 mM) and
148 MiliQ water. Technical triplicates of each biological replicate were performed. The amplifications were
149 carried out with the following cycling parameters: an initial heating to 95 °C (5 min), followed by 40
150 cycles (16S rRNA) or 50 cycles (PAH-RHDαGN and C203). These cycles consisted of 30s of denaturation
151 at 95 °C, 30s at the primer's specific annealing temperature (53°C for 16S rRNA and 57°C for GN PAH-
152 RHDα and C230) and 30s of elongation at 72 °C. The final step was for 7 min at 72 °C. Melting curve
153 analyses were carried out to dismiss contamination. Sample gene-copy number was determined using
154 standard curves built from serial dilutions of gene-target specific plasmids.

155 **2.6 Sequencing Analysis**

156 Total DNA of day 0 of control microcosms, and day 15 and 58 samples of all treatments were selected
157 to analyze bacterial community composition using V4 hypervariable region of bacterial 16S rRNA gene
158 using universal primer set 515F (GTGCCAGCMGCCGCGGTAA) 806R (GGACTACHVGGGTWTCTAAT).
159 Sample sequencing was performed using Illumina NovaSeq 6000 platform at Novogene Company.
160 Paired end sequencing data was analyzed using QIIME 2 (v2022.2) (Bolyen et al., 2019). Raw data was
161 filtered followed by denoising with DADA2 to obtain Amplicon Sequence variants (ASV). Taxonomy was
162 assigned using SILVA v.138 trained database.
163 To follow the behavior of inoculated strains, the ASVs with higher sequence identity with the 16S rRNA
164 gene sequence for each strain were identified using BLASTn database. These ASV were used to
165 calculate their contribution of each strain to its respective genus.
166 Alpha diversity metrics (Chao1, Shannon and Faith's Phylogenetic Diversity) were estimated using q2-
167 diversity after samples were rarefied to 72046 reads per sample. Further analyses were carried out in
168 the R environment. Beta diversity was analyzed through a Principal Coordinates Analysis (PCoA) using
169 Bray-Curtis dissimilarity index at ASV level, performed with the *phyloseq* (v.1.42.0) and vegan (v.2.6-4)
170 R packages. PICRUSt2 software was utilized to predict the abundance of gene families KEGG (Kyoto
171 Encyclopedia of Genes and Genomes) orthologs (KOs) (Douglas et al., 2020). Differential abundance
172 analysis of both taxonomy (at genus level) and functions (at KO level) were carried out using ANCOM-
173 BC (v2.0.0) R package (Lin and Peddada, 2020). A prevalence filter of 0.1, a significance of $p<0.05$ and
174 multiple pairwise comparison considering the mdFDR, using holm as adjusted method.
175 To create the co-occurrence networks for each study, ASVs tables were filtered with relative
176 abundance above 0.5 %. Correlation Network Analysis was performed using Sparse Co-occurrence
177 Network Investigation for Compositional data (SCNIC) integrated in the q2-scnic plugin from Qiime2
178 software toolkit. From correlations matrix the networks were constructed with a minimum of R
179 correlation- value cutoff of 0.50 (p-value 0.01). For each microbial network, topological parameters
180 were measured by Network Analyzer plugin in Cytoscape v3.7.9. Positively interconnected ASVs were
181 identified and visualized using Gephi v0.10.

182 **2.7 Statistical Analysis**

183 Statistical analysis of PAH concentration and diversity indexes were performed through mixed ANOVA.
184 Normality and homogeneity of variances assumptions were checked through Shapiro-Wilk and Levene
185 test, respectively. Pairwise comparisons were corrected using Benjamini-Hochman method. All the
186 tests were performed using *rstatix* (v.0.7.2) R package.

187 **2.8 Data deposition**

188 The raw data sequence for 16S rRNA gene amplicons have been deposited under NCBI accession
189 number PRJNA889803.

190

191 **3 Results**

192 **3.1 Degradation of supplemented PAHs**

193 Degradation efficiency of the bioaugmentation process with the three different consortia was
194 evaluated by analyzing the remaining concentration of the supplemented PAHs (fluorene,
195 phenanthrene, anthracene and pyrene) along incubation time (0, 15, 30 and 58 days) in the
196 microcosms inoculated with SC AMBk, SC1 and SC4 consortia as well as in SP+PAH (contaminated
197 control without inoculation). Results are shown in figure 1. The non-contaminated control (control)
198 was excluded from this figure along with day 58 of all treatments, as PAHs concentration was below
199 the detection limit.

200 A significant decrease ($p<0.05$) of the supplemented PAHs was observed on day 15 of incubation in the
201 inoculated microcosms. Fluorene, anthracene and phenanthrene removal was greater than 99%, with
202 no significant differences between these microcosms. Pyrene degradation was significantly higher
203 ($p<0.05$) in SC AMBk inoculated microcosms (42% degradation was achieved) compared to those
204 inoculated with SC1 (19%). While no degradation of the supplemented PAHs was observed after 15
205 days of incubation in SP+PAH, a complete elimination of fluorene, 97% degradation of phenanthrene,
206 92% anthracene and 46% pyrene were measured after 30 days of incubation. At this point, low
207 molecular weight PAH concentration in the inoculated microcosms was under the quantification limit,

208 while in SP+PAH remaining concentrations of 12.5 mg. Kg-1 of dry soil for phenanthrene and 5.14 mg.
209 Kg-1 of dry soil for anthracene were detected.
210 Concentration of all PAH was below the detection limit in all the studied microcosms at the end of the
211 incubation period (day 58).
212
213 **3.2 Population dynamics and quantification of specific genes related with PAH degradation by qPCR**
214 The dynamics and the degrading potential of soil bacterial populations in the community were
215 assessed by qPCR of the 16S rRNA gene and of two specific genes related: the PAH-RHDα GN gene, and
216 the C230 gene.
217 The copy number of the 16S rRNA gene for all microcosms during the incubation time was around 10^9-
218 10^{10} copies.g^{-1} of dry soil. In order to normalize the variations in the copy number of specific genes, a
219 percentage ratio was calculated using the copy number value of each specific gene compared to the
220 one of 16S rRNA gene. Figure 2 shows these gene ratios over time for the different microcosms. No
221 differential pattern was observed in the C230 gene/16S rRNA gene ratio during the incubation period
222 or between microcosms. However, in the inoculated microcosms, the PAH-RHDα GN/16S rRNA ratio
223 was higher than the control and SP+PAH on day 0. After 30 days of incubation this ratio increased its
224 value in SP+PAH reaching similar values to the ones obtained for inoculated microcosms. At the end of
225 the incubation period the PAH-RHDα GN/16S rRNA ratio was similar for all microcosms.
226
227 **3.3 Analysis of the soil microbiome diversity**
228 The inoculation effect on bacterial community structure during the bioaugmentation process was
229 studied through 16S rRNA gene metabarcoding at different times of incubation. Time points were
230 selected considering the observed PAH elimination kinetics (day 15 and 58 for all treatments and day
231 0 only for the control).
232 Alpha diversity analysis was carried out applying Chao1, Shannon and Faith indexes (Figure S2). The
233 control microcosms showed an increase in these index values on day 15, being significantly higher than

234 the inoculated microcosms. At the end of the incubation period, no differences were observed among
235 all systems.
236 Beta diversity analysis showed that inoculation had a remarkable effect on community structure during
237 the first days of incubation (Figure S3), while a convergence in the community structure was observed
238 between inoculated and control microcosms at the end of incubation period.
239
240 **3.4 Composition of the soil microbiomes and monitoring of the inoculated strains**
241 Five predominant phyla were identified in the microcosms on day 15 of incubation: Proteobacteria
242 (32%), Actinobacteriota (15%) Acidobacteriota (7%) and Verrucomicrobiota (6%).
243 Table S1 and Figure 3 show the relative abundance of the bacterial orders at the different incubation
244 times. After 15 days, Galelialles order (8%, Actinobacteriota phylum) was predominant in the control
245 microcosms, followed by the Nitrososphaerales order (6%, Crenarchaeota phylum). In all
246 contaminated microcosms, an increase in Proteobacteria was observed compared to day 0. While its
247 relative abundance in the inoculated microcosmos was 50%, in SP+PAH and control microcosms was
248 37% and 21% respectively. Within this phylum, Burkholderiales was the predominant order in the
249 microcosms inoculated with SC AMBk, SC4 and in SP+PAH. At genus level, while *Burkholderia-*
250 *Caballeronia-Paraburkholderia* were the most abundant genera in the SC AMBk and SC4 inoculated
251 microcosms, reaching a relative abundance value of 16% in both systems, it represented only 3.5% in
252 SC1 inoculated microcosms, and did not exceed 1% in the SP+PAH and control microcosms. The ASV
253 identified for Bk (Table S2) contributed to more than 90% to these genera in SC AMBk and SC4
254 inoculated microcosms, while represented less than 50% in the other microcosms. Within the
255 mentioned order, *Cupriavidus* was a predominant genus in SP+PAH microcosms (15%), reaching
256 relative abundances lower than 4% in the inoculated microcosms, while it did not exceed 1 % in the
257 control microcosms.
258 In SC1 inoculated microcosms, Sphingomonadales (Proteobacteria) and Chthoniobacterales
259 (Verrucomicrobiota) were predominant orders, both with relative abundances of 14%. Within the

former order, while *Sphingobium* and *Sphingomonas* were major genera in the inoculated microcosms, showing abundances greater than 4% and 5%, respectively, in the SP+PAH microcosms their relative abundances were 1% and 3% respectively. The ASV identified as AM strain (Table S2) was present in almost all microcosms but its contribution to *Sphingobium* genus was more than 99% in the inoculated microcosms. Regarding Chthoniobacterales members, *Candidatus Udeobacter* was the predominant genus (13%) in the SC1 inoculated microcosms and was the second most abundant in the microcosms inoculated with SC4 (9%), SC AMBk (7%) and in the SP+PAH (6%) and control (5%) microcosms.

Among other predominant genera, while *Acinetobacter* (order Pseudomonadales) showed a relative abundance greater than 3% in the SC1 and SC4 inoculated microcosms, in the remaining microcosms it did not exceed values of 0.5%. *Inquilinus* (order Azospirilales) was found in SC1 inoculated microcosms with a relative abundance of 4% at 15 days of incubation, although it did not exceed 1% in the other analyzed microcosms. The ASV identified as Inq strain contributed more than 90% to this genus.

The predominance of Proteobacteria was also observed at day 58 of incubation, in the contaminated microcosms (42-47%), followed by Verrucomicrobiota (13-18%). In contaminated microcosms, *Candidatus Udeobacter* was the predominant genus (12-17%), followed by *Sphingomonas* (9-11%) and *Sulfuritalea* (order Burkholderiales) (5-10%).

Regarding to the control, an increase of the relative abundance of *Candidatus Udeobacter* was observed (16%) compared to day 15, which was the major genus, followed by an unclassified genus from the Nitrososphaeraceae family (13%).

3.5 Analysis of Compositions of Microbiomes with Bias Correction (ANCOM-BC)

A differential abundance analysis on bacterial genera was performed using the ANCOM-BC methodology (Lin and Peddada, 2020). This methodology considers the compositional nature of the sequencing data, uses absolute abundances, estimates the sample fraction, and performs a theoretical

285 correction for the bias associated with this fraction between samples. In order to obtain robust results,
286 the analysis focused on those genera that exceed a prevalence of 10% (Nearing et al., 2022).
287 Figure 4 shows the differentially abundant genera in the analyzed microcosms at 15 and 58 days of
288 incubation.
289 After 15 days of incubation, 38 bacterial genera resulted differentially abundant, representing a minor
290 percentage of the total genus found (7%) (Figure 4).
291 When comparing SP+PAH with control microcosms, 3 genera showed significantly higher abundances
292 in the former: *Cupriavidus* (lfc 3.8, Burkholderiales), a genus from the *Rhodanobacteracea* family and
293 *Dyllela* (lfc 1.8 and lfc 1.6 respectively, Xanthomonadales). However, higher differences were observed
294 between the inoculated and the control microcosms. SC1 inoculated microcosms showed the highest
295 number of differentially abundant genera, 21 genera with higher abundance than the control. Among
296 these, major changes were observed for *Inquilinus* (lfc 4.6, Azospirillales), *Sphingobium* (lfc 4.0,
297 Sphingomonadales), and an unclassified genus of the family Rhodobactereaceae (lfc 2.7,
298 Rhodobacterales). 12 genera showed lower abundances in SC1 than in the control, and among them
299 were *Adhaeribacter* (lfc -2.7, Cytophagales), *Devosia* (lfc -2.4, Hyphomicrobiales) and *BIrii41* (lfc -2.2,
300 Polyangiales).
301 SC AMBk and SC4 inoculated microcosms showed 14 differentially more abundant genera compared
302 to the control, with 10 of them showing the same behavior. Two of the most abundant genera were
303 *Sphingobium* and *Burkholderia-Caballeronia-Paraburkholderia* (Bukholderiales) (lfc 3.3-3.4 and lfc 3.8
304 respectively). When focusing on the genera being differentially less abundant in SC AMBk and SC4
305 compared to the control, a non-cultivable genus of the Microscillaceae family (lfc -4.9) and
306 *Streptococcus* (lfc -3.6, Lactobacillales) was found for the SC4 comparison and *Sulfiritalea* (lfc -4.8,
307 Burkholderiales) for the SC AMBk one.
308 Seven genera were found to be significantly more abundant in the 3 inoculated microcosm compared
309 to the control, *Sphingobium* and *Sphingomonas* (Sphingomonadales), *Aeromicrobium*
310 (Propionibacteriales), *Chthoniobacter* (Chthoniobacterales), *Burkholderia—Caballeronia-*

311 *Paraburkholderia* and *Cupriavidus* (Burkholderiales) and *Dyella* (Xanthomonadales), while 3 genera
312 showed lower abundances in these microcosms, *Birii41* (Polyangiales), *Acidibacter* and a non-
313 cultivable genus from the Microscillaceae family.
314 When comparing the inoculated microcosms with SP+PAH, the SC1, SC4 and SC AMBk inoculated
315 microcosms showed 17, 9 and 8 differentially abundant genera, respectively. Although most of these
316 genera behaved similarly to what was observed in the comparison between inoculated and control
317 microcosms, some genera showed unique variation in relation to SP+PAH. For example, a higher
318 abundance of a genus of the Oxalobacteracea family (Burkholderiales) was observed in SC1 (lfc 3.8)
319 and in SC4 (lfc 4.1) inoculated microcosms compared to SP+PAH. Among the genera that showed
320 significantly lower abundances in relation to SP+PAH, *Cupriavidus* was found in the microcosms with
321 SC AMBk (lfc -1.6) and SC4 (lfc -1.8) and *Kribbella* (Propionobacterales) was found in the microcosms
322 with SC1 (lfc -1.2) and SC4 (lfc -1.1).
323 When comparing the different inoculants, only *Burkholderia-Caballeronia-Paraburkholderia* (lfc -1.1)
324 and a non-cultivable genus of the Sandaracinaceae family (lfc -3.6) showed significantly lower
325 abundances in the SC1 compared SC AMBk inoculated microcosms. No differentially abundant genera
326 were observed when comparing SC4 microcosms with SC1 or SC AMBk microcosms.
327 At 58 days of incubation, 2% of the total bacterial genera (12 genera) showed significant changes in
328 the comparisons (Figure 4). Only 3 differentially abundant genera were found between the inoculated
329 microcosms and the control, being one of them *Sulfuritalea* (lfc 7.7, 8.5 and 8.9 for SC1, SC4 and SC
330 AMBk respectively). SP+PAH microcosms showed a total of 4 significantly more abundant genera
331 compared to the control: *Sulfuritalea* (lfc 6.9), *Sphingomonas* (lfc 1.3), an unclassified genus of the
332 Oxalobactereaceae family (lfc 5.4) and a non-cultivable genus of the Moraxellaceae family (lfc 2.5).
333 In relation to the inoculated microcosms, SP+PAH showed significantly higher abundances
334 *Burkholderia-Caballeronia-Paraburkholderia* and *Sphingobium* genera at 58 days of incubation.
335

336 **3.6 Functional prediction by PICRUST and contribution of the different genera to the KOs related to**
337 **PAH degradation**

338 The functional potential of the bacterial community of each treatment was predicted using PICRUSt2
339 software. The reliability of this prediction was evaluated by analyzing NSTI values, resulting in an
340 average of 0.21±0.03 for all treatments (Table S3). A total of 7605 KOs were found in the dataset, but
341 only 167 were related to the degradation of aromatic compounds. In order to evaluate which of these
342 KO were differentially abundant in each treatment along the incubation time, ANCOM-BC method was
343 applied performing different comparisons.

344 The Figure S4 shows the comparison between treatments after 15 and 58 days of incubation which
345 resulted in 73 and 19 differentially abundant KO, respectively.

346 Regarding the comparison at day 15 with SP+PAH, 16 KO were found to be differentially more
347 abundant in SC1 and 10 KO in SC4 and SC AMBk. Seven of these KO were common to the inoculated
348 microcosms and were related to the first steps of the PAH degradation pathway (K14581) and the
349 ortho-cleavage of central intermediates (K00455, K04100, K04101, K05921 and K10219). Furthermore,
350 several KO were found to be significantly more abundant in SP+PAH than in the inoculated
351 microcosms; 15 of these KO were shared between the three inoculated microcosms and were related
352 to toluene (K00055, K15760, K15761, K15762, K15763, K15764, K15765), benzoate (K07535, K07536,
353 K10621, K10622) and phthalate (K18068) degradation.

354 In the comparisons within the inoculated microcosms, only 3 KO resulted significantly less abundant
355 in SC AMBk than in SC1, but no difference was found between SC4 and SC1 or SC AMBk.

356 At day 58 of incubation, only one KO (K14581) was significantly more abundant in SP+PAH than in the
357 non-contaminated control and no differences were found in the comparison including the inoculants.

358 The genera contribution to the eight more differentially abundant KO shared among the inoculated
359 microcosm at day 15 were evaluated considering their participation in upper and the lower
360 degradation pathway (Figure 5). For this analysis only the genera contributing in more than 5% in at
361 least one condition were selected. Notably, in the chord diagrams of the inoculated microcosms (Figure

362 5) *Sphingobium* and *Burkholderia* were the genera that contributed more to the eight analyzed KO.
363 Those related to protocatechuate degradation were mostly assigned to *Sphingobium* (K10219, K04100,
364 K04101 and K11949) and *Burkholderia* represented a minor fraction in the contribution. However, the
365 ones related to 3,4-dihydroxyphenylacetate and benzoate degradation were assigned to *Burkholderia*
366 (K14581, K00455, K05921 and K00141) and no contribution of *Sphingobium* was found in those KO.
367 *Pseudomonas*, *Cupriavidus*, *Acidothermus*, *Reynella* and *Bradirhizobium* genera were also predicted to
368 contribute to the analyzed KO and their contribution was higher in SC1 than in the other treatments
369 (Figure 5).
370
371 **3.7 Soil microbiomes co-occurrence networks**
372 A network analysis was adopted to explore the effects of addition of contaminants and
373 bioaugmentation within soil bacterial interactions. Properties of each resultant network are
374 summarized in Table 1. At day 15 of incubation a decrease in the number of the predicted interactions
375 was observed within the soil bacterial community members due to PAH supplementation, since
376 SP+PAH, as regards to the non-contaminated control, presented a reduction of 38% (from 725 to 450)
377 of total interactions. This reduction was accompanied by a change in the structural features, nodes
378 and edges of bacterial networks as the path length increased and the cluster coefficient and network
379 density decreased, showing that it was a less connected community with more alienated relationships,
380 compared to the control (Table 1 and Figure 6).
381 When comparing the inoculated microcosms with the SP+PAH microcosms, on day 15, higher number
382 of interactions was observed in the latter, but this decrease is mainly due to the decrease in negative
383 interactions (around 40 to 70 %).
384 In all inoculated microcosms, positive interactions were predicted between the orders of the
385 inoculated microorganisms and Propionibacteriales. Also, positive interactions were found in SC1 and
386 SC4 inoculated microcosms with Xanthomonadales (Figure 6).

387 Regarding the co-occurrence networks of the inoculated microcosms, SC AMBk and SC4 resultant
388 networks possessed the shortest average path length, the highest cluster coefficient and network
389 density (Table 1), indicating closer relationships of soil microbial taxa.
390 At the end of the incubation time, all the co-occurrence networks had a higher density value, higher
391 clustering coefficient and shorter path length value compared to those of the day 15, indicating that
392 the nodes had a higher degree of interaction and association when the contaminant concentration and
393 inoculants members decreased.
394 The number of orders identified as keystone varied between treatments and incubation time.
395 However, common keystone taxa were found in the contaminated and inoculated microcosms, such
396 as Gaiellales, Gemmantimonadales, Actinomycetales, Solirubrobacterales and Sphigomonadales,.
397 In addition, to study the interactions existing prior to inoculation, a network for SP+PAH microcosms
398 at genus level was constructed (Figure S5). In this network interactions between soil bacterial residents
399 and *Burkholderia-Caballeronia-Paraburkholderia* were analyzed. As a result, negative interactions
400 were found with *Cupriavidus, Dyella* and *Sulfuritalea* genera and positive interactions with
401 *Aeromicrobium, Gaiella* and *Sphingomonas* genera.
402

403 **4. Discussion**

404 With an increasing focus on microbiome engineering, understanding and manipulating complex
405 microbial ecosystems has become a defining mission for microbiome science (Kong et al., 2018). Our
406 study provides insights into the structure, dynamics, and ecology of interacting microbial species
407 during inoculation of allochthonous microorganisms capable of removing contaminants, which is a
408 promising strategy in bioremediation of acutely contaminated soils (Nwankwegu et al., 2022).
409 The bioaugmentation with three consortia used in this work stimulated the degradation of the mixture
410 of PAHs supplemented to the soil, reaching the complete elimination of low molecular weight PAHs
411 and partial degradation of high molecular weight PAH already at 15 days of incubation (Figure 1). The
412 higher biodegradation potential of PAH (number of copies of the PAH RHDα-GN), observed in the

413 inoculated microcosms compared to SP+PAH and control microcosms (Figure 2), was expected due to
414 the introduction of the inoculants that contain those genes in their genomes (Macchi et al., 2021).
415 These results were reinforced by the functional prediction carried out by PICRUSt2 (Figure 4 and 5),
416 where the inoculated genera *Sphingobium* and *Burkholderia* contributed more to the KOs that showed
417 higher abundance than SP+PAH and control microcosms, highlighting their main role on PAH
418 degradation among the consortium members. Within these KOs, K14581 (naphthalene 1,2-
419 dioxygenase ferredoxin reductase component) could act in the first steps of the degradation of PAHs
420 (fluorene, anthracene, benzo[a]pyrene and pyrene) (Zhou et al., 2020) with *Burkholderia* genus
421 contributing the most. Expression of this enzyme by Bk was observed during the degradation of
422 phenanthrene in liquid media, both in SC-4 and in SC AMBk (Macchi et al., 2021; Nieto et al., 2023).
423 This could be related to the higher pyrene degradation found in SC AMBk inoculated microcosms at 15
424 days of incubation (Figure 1). Several KOs linked to the degradation of protocatechuate (K04100,
425 K04101, K10219, K00455), a metabolite of PAH degradation, showed higher abundances in the
426 inoculated microcosms, which could indicate the predominance of the ortho-cleavage pathway (Figure
427 S4). Other authors also reported an increase in specific functions associated with inocula in
428 bioaugmentation studies (Cayetano et al., 2021; Zhou et al., 2022).
429 Microbial community in SP+PAH microcosms were also able to degrade the supplemented PAH;
430 however, this process, unlike the inoculated microcosms, was delayed until day 30 (Figure 1). This
431 could be the result of selecting native degrading microorganisms made by pollutants, consistent with
432 the increase of PAH RHDα-GN gene after 30 days of incubation. No differences were observed in C230
433 gene copy number between the inoculated microcosms and the control microcosms, probably due to
434 the participation of this gene in other metabolic pathways involving one-ring aromatic compounds.
435 Bioaugmentation failure could result from consortia selected under laboratory conditions becoming
436 less competitive under harsh and/or variable field conditions (Palkova, 2004; Steensels et al., 2019).
437 Hence, following the survival of the inoculum is key to understand the success of bioaugmentation
438 process. *Sphingobium* and *Burkholderia* were both members of SC AMBk and SC4 consortia and were

439 found to be among the predominant genera in the microcosms inoculated with these consortia at 15
440 days of incubation. A significant increase of *Burkholderia* abundance was also observed in the SC1
441 inoculated microcosms in comparison to SP+PAH, even though this genus is not a member of this
442 consortium; this behavior would indicate mutualistic interactions between *Sphingobium* and
443 *Burkholderia*, which were also previously reported (Zhang et al., 2013; Willsey and Wargo, 2015; Festa
444 et al., 2016a).
445 A recent metanalysis showed that inoculant diversity correlates significantly and positively with
446 inoculum effect (Liu et al., 2023). One explanation could be that more species in a consortium increase
447 its multifunctionality and stability (Jiménez et al., 2018). However, our results did not show differences
448 between the different inoculants, demonstrating that a more diverse consortia will not always lead to
449 an improvement in the degradation performance. In our study, *Sphingobium* and *Burkholderia* played
450 a main role in PAH-degradation, which might be related to the changes in resource availability due to
451 the PAHs addition to the soil. Thus, *Sphingobium* and *Burkholderia* may have taken advantage of this
452 open niche, outcompeting the native community and increasing their establishment success.
453 (Silverstein et al., 2023).
454 On the other hand, the rest of consortium members are known to play a major role in the lower PAH-
455 degradation pathway (Macchi et al., 2021), whose enzymes are more widespread in nature than the
456 ones in the higher PAH-degradation pathway and could act in other several metabolic pathways.
457 Therefore, the absence of establishment of the other consortium members could be a consequence of
458 their competition with the high diverse native community (Figure S2 and 3), since the remaining niche
459 available, related to PAH intermediate degradation, decreased (Mallon et al., 2015). In this scenario
460 with high resource availability, bioaugmentation efficiency relayed on those consortium members with
461 key catabolic functionalities (i.e., *Sphingobium* and *Burkholderia*), while further degradation of the
462 intermediates, which involve fewer specific functions, could be carried out by the native
463 microorganism. The ability of *Sphingobium* AM as a sole strain to establish and increase the soil
464 biodegradation activity was previously observed (Festa et la., 2016a) when applied as inoculant in an

465 acutely contaminated soil. However, in that study the inoculation produced drastic changes in the
466 structure and diversity of soil bacterial community that remained even after 63 days of incubation.
467 Moreover, it becomes essential to study the interaction between the inoculants and the native
468 community, since the efficiency of the process depends on the survival of the inoculant but, at the
469 same time, the least impact is sought on the structure and functionality of the native community
470 (Mawarda et al., 2020) after the bioremediation process is complete.
471 Incubation conditions had a stimulating effect on the bacterial populations of the control microcosms,
472 evidenced by the increase in both richness and diversity at 15 days of incubation. This effect, previously
473 observed in other bioaugmentation processes, was not found in the inoculated microcosms (Figure
474 S2), which could be mainly linked to the predominance of the inoculants (Festa et al., 2016b;
475 Chaudhary et al., 2021; Zhou et al., 2022). In turn, Faith's index showed a significant decrease in the
476 inoculated microcosms regarding the control and SP+PAH microcosms, probably indicating that
477 inoculation generated a rapid change in the bacterial community towards microorganisms whose
478 phylogenetic relationship was greater. The β diversity analysis also showed an early impact of
479 inoculation on the bacterial community structure (Figure S3).
480 Co-occurrence networks of the inoculated microcosms (Figure 6) at day 15 showed a lower number of
481 total interactions than in SP+PAH, possibly due to a reorganization of interactions caused by the
482 inocula. Inoculation resulted in a higher decrease in negative than in positive interactions (Table 1)
483 which correlates with bioaugmentation effectiveness, since negative interactions of an inoculant with
484 other soil microorganisms can produce a delay in the effect of bioaugmentation (Jiang et al., 2022).
485 Changes in community structure were observed as a consequence of both inoculation and
486 contamination. As previously discussed, a selection of PAH-degrading microorganisms was observed
487 in SP+PAH microcosms. As in the inoculated microcosms, Proteobacteria was the main phylum, with a
488 predominance of Burkholderiales order. While the predominant genus in SP+PAH microcosms was
489 *Cupriavidus*, in SC AMBk and SC4 inoculated microcosms its abundance was significantly lower
490 compared to SP+PAH (Figure 3). This could be a consequence of the predominance of *Burkholderia* in

491 inoculated microcosms, since both genera have a similar catabolic potential (Pérez-Pantoja et al., 2012)
492 and could compete for resources, where the predominance of one could limit the growth of the other.
493 Competition between the genera *Cupriavidus* and *Burkholderia* was inferred in the correlation
494 networks of the contaminated system (Figure S5).
495 Common effects on the soil bacterial community were observed beyond the behavior of the inoculated
496 genera. A predominance of the Proteobacteria phylum (Table S1) was found, which includes several
497 PAH-degrading members. The genera *Aeromicrobium* (Propionobacteriales) and *Nevskia*
498 (Xanthomonadales) showed higher abundances in the inoculated microcosms compared to SP+PAH
499 and control microcosms. Members of these genera were reported to have direct participation in PAH
500 degradation (Crampon et al., 2018; Li et al., 2021). In addition, positive interactions were predicted
501 between the inoculated orders and members of the autochthonous orders potentially involved in PAH
502 degradation such as Propionibacteriales and Xanthomonadales order (Figure 6). Indeed, all the
503 bacterial orders that were indicated as keystone in most of the treatments, meaning they play a key
504 role in modulating network structure and function, were orders with known PAHs-degrading
505 capabilities (Pagé et al., 2015; Zhang et al., 2022).
506 The structural and functional divergence between the microbiome of the control and the
507 contaminated microcosms decreased at 58 days of incubation with no significant differences observed
508 in diversity indices (Figure S2) and reduced number of differentially abundant genera and functions
509 (Figure 3 and S4). At this time, the increase in network connections and microbial interactions was
510 observed (Table 1), which could indicate a more stable microbial community as more connected
511 networks could have higher community stability and resistance to disturbances (de Vries et al., 2018).
512 When referring to the observed differentially abundant genera at 58 days of incubation, *Sulfuritalea*,
513 a genus found in PAH-contaminated soils (Guo et al., 2017; Yang et al., 2022), was significantly higher
514 in the contaminated microcosms than in the control microcosms (Figure 3 and 4). This genus was
515 pointed as indicator taxa, tolerant to hydrocarbon, potentially involved in hydrocarbon-degradation or
516 benefiting from the degradation by-products (Cébron et al., 2022). Its presence in the contaminated

microcosms at day 58 could be linked to a residual effect of the contamination. However, in all microcosms, a predominance of *Candidatus Udaeobacter* was found at the end of the incubation period, one of the most abundant soil bacteria with global dissemination (Brewer et al., 2016; Willms et al., 2020), whose abundance correlates with soil health (Wilhelm et al., 2023).

Results obtained in this work show that the new microbiome assembly achieved through bioaugmentation with the three degrading consortia not only increases the metabolic capacities of the microbiome due to the added microorganisms, but also stimulates the native degrading populations of the soil. At the same time, at the end of the incubation period, the impact of the inoculation was reduced as all the microbiomes converged with the non-contaminated control microcosms (Figure 3, 4 and 5; Table S1).

5.Conclusion

The three inoculated consortia were successful in accelerate the removal of contaminants. As long as the inoculant has the capacity to initiate the PAH degradation, competitiveness and efficiency of the inoculant does not depend on its diversity in cases of acutely contaminated soils with PAHs of up to four rings. Furthermore, an increase in the abundance of bacterial genera related to soil health was observed at the end of the of the incubation period. Our results show a significant advantage of inoculation with allochthonous microorganisms since temporary establishment of the inoculant and its low impact on the native microbiota are desired objectives in inoculation processes.

6. Funding information

This research was partially supported by the Agencia Nacional de Promoción Científica y Tecnológica (ANPCyT), Argentina; (PICT 2013–1805). Nieto E. has doctoral fellowship supported by Consejo Nacional de Investigaciones Científicas y Técnicas (CONICET), Argentina. Coppotelli B.M. and Festa S. are research members of CONICET. Morelli I.S. is a research member of CIC-PBA. Colman D. is technical support member of CONICET.

7. Declaration of Competing Interest

The authors declare that they have no known competing financial interests or personal relationships that could have appeared to influence the work reported in this paper.

8. References

Abdel-Shafy, H.I., Mansour, M.S.M., 2016. A review on polycyclic aromatic hydrocarbons: Source, environmental impact, effect on human health and remediation. Egyptian Journal of Petroleum. https://doi.org/10.1016/j.ejpe.2015.03.011

Albright, M.B.N., Louca, S., Winkler, D.E., Feeser, K.L., Haig, S.J., Whiteson, K.L., Emerson, J.B., Dunbar, J., 2022. Solutions in microbiome engineering: prioritizing barriers to organism establishment. ISME Journal. https://doi.org/10.1038/s41396-021-01088-5

Bolyen, E., Rideout, J.R., Dillon, M.R., Bokulich, N.A., Abnet, C.C., Al-Ghalith, G.A., Alexander, H., Alm, E.J., Arumugam, M., Asnicar, F., Bai, Y., Bisanz, J.E., Bittinger, K., Brejnrod, A., Brislawn, C.J., Brown, C.T., Callahan, B.J., Caraballo-Rodríguez, A.M., Chase, J., Cope, E.K., Da Silva, R., Diener, C., Dorrestein, P.C., Douglas, G.M., Durall, D.M., Duvallet, C., Edwardson, C.F., Ernst, M., Estaki, M., Fouquier, J., Gauglitz, J.M., Gibbons, S.M., Gibson, D.L., Gonzalez, A., Gorlick, K., Guo, J., Hillmann, B., Holmes, S., Holste, H., Huttenhower, C., Huttley, G.A., Janssen, S., Jarmusch, A.K., Jiang, L., Kaehler, B.D., Kang, K. Bin, Keefe, C.R., Keim, P., Kelley, S.T., Knights, D., Koester, I., Kosciolek, T., Kreps, J., Langille, M.G.I., Lee, J., Ley, R., Liu, Y.-X., Loftfield, E., Lozupone, C., Maher, M., Marotz, C., Martin, B.D., McDonald, D., McIver, L.J., Melnik, A. V., Metcalf, J.L., Morgan, S.C., Morton, J.T., Naimey, A.T., Navas-Molina, J.A., Nothias, L.F., Orchanian, S.B., Pearson, T., Peoples, S.L., Petras, D., Preuss, M.L., Pruesse, E., Rasmussen, L.B., Rivers, A., Robeson, M.S., Rosenthal, P., Segata, N., Shaffer, M., Shiffer, A., Sinha, R., Song, S.J., Spear, J.R., Swafford, A.D., Thompson, L.R., Torres, P.J., Trinh, P., Tripathi, A., Turnbaugh, P.J., Ul-Hasan, S., van der Hooft, J.J.J., Vargas, F., Vázquez-Baeza, Y., Vogtmann, E., von Hippel, M., Walters, W., Wan, Y., Wang, M., Warren, J., Weber, K.C., Williamson, C.H.D., Willis, A.D., Xu, Z.Z., Zaneveld, J.R., Zhang, Y., Zhu, Q., Knight, R., Caporaso, J.G., 2019. Reproducible, interactive, scalable and extensible microbiome data science using QIIME 2. Nat Biotechnol 37, 852–857. https://doi.org/10.1038/s41587-019-0209-9

Brewer, T.E., Handley, K.M., Carini, P., Gilbert, J.A., Fierer, N., 2016. Genome reduction in an abundant and ubiquitous soil bacterium “Candidatus Udaeobacter copiosus.” Nat Microbiol 2. https://doi.org/10.1038/nmicrobiol.2016.198

Cayetano, R.D.A., Park, J., Kim, G.B., Jung, J.H., Kim, S.H., 2021. Enhanced anaerobic digestion of waste-activated sludge via bioaugmentation strategy—Phylogenetic investigation of communities by reconstruction of unobserved states (PICRUSt2) analysis through hydrolytic enzymes and possible linkage to system performance. Bioresour Technol 332. https://doi.org/10.1016/j.biortech.2021.125014

Cébron, A., Borreca, A., Beguiristain, T., Biache, C., Faure, P., 2022. Taxonomic and functional trait-based approaches suggest that aerobic and anaerobic soil microorganisms allow the natural attenuation of oil from natural seeps. Sci Rep 12. https://doi.org/10.1038/s41598-022-10850-4

583 Chaudhary, D.K., Bajagain, R., Jeong, S.W., Kim, J., 2021. Effect of consortium bioaugmentation and
584 biostimulation on remediation efficiency and bacterial diversity of diesel-contaminated aged
585 soil. World J Microbiol Biotechnol 37. https://doi.org/10.1007/s11274-021-02999-3

586 Che, S., Men, Y., 2019. Synthetic microbial consortia for biosynthesis and biodegradation: promises
587 and challenges. J Ind Microbiol Biotechnol 46, 1343–1358. https://doi.org/10.1007/s10295-019-
588 02211-4

589 Cornell, C., Kokkoris, V., Richards, A., Horst, C., Rosa, D., Bennett, J.A., Hart, M.M., 2021. Do
590 Bioinoculants Affect Resident Microbial Communities? A Meta-Analysis. Frontiers in Agronomy.
591 https://doi.org/10.3389/fagro.2021.753474

592 Crampon, M., Bodilis, J., Portet-Koltalo, F., 2018. Linking initial soil bacterial diversity and polycyclic
593 aromatic hydrocarbons (PAHs) degradation potential. J Hazard Mater 359, 500–509.
594 https://doi.org/10.1016/j.jhazmat.2018.07.088

595 de Vries, F.T., Griffiths, R.I., Bailey, M., Craig, H., Girlanda, M., Gweon, H.S., Hallin, S., Kaisermann, A.,
596 Keith, A.M., Kretzschmar, M., Lemanceau, P., Lumini, E., Mason, K.E., Oliver, A., Ostle, N.,
597 Prosser, J.I., Thion, C., Thomson, B., Bardgett, R.D., 2018. Soil bacterial networks are less stable
598 under drought than fungal networks. Nat Commun 9. https://doi.org/10.1038/s41467-018-
599 05516-7

600 Douglas, G.M., Maffei, V.J., Zaneveld, J.R., Yurgel, S.N., Brown, J.R., Taylor, C.M., Huttenhower, C.,
601 Langille, M.G.I., 2020. PICRUSt2 for prediction of metagenome functions. Nat Biotechnol.
602 https://doi.org/10.1038/s41587-020-0550-z

603 Fath, B.D., Scharler, U.M., Ulanowicz, R.E., Hannon, B., 2007. Ecological network analysis: network
604 construction. Ecol Modell 208, 49–55. https://doi.org/10.1016/j.ecolmodel.2007.04.029

605 Festa, S., Coppotelli, B.M., Morelli, Irma.S., 2016a. Comparative bioaugmentation with a consortium
606 and a single strain in a phenanthrene-contaminated soil: Impact on the bacterial community
607 and biodegradation. Applied Soil Ecology 98, 8–19.
608 https://doi.org/10.1016/j.apsoil.2015.08.025

609 Festa, S., Coppotelli, B.M., Morelli, I.S., 2016b. Comparative bioaugmentation with a consortium and
610 a single strain in a phenanthrene-contaminated soil: Impact on the bacterial community and
611 biodegradation. Applied Soil Ecology 98, 8–19. https://doi.org/10.1016/j.apsoil.2015.08.025

612 Festa, S., Coppotelli, B.M., Morelli, I.S., 2013. Bacterial diversity and functional interactions between
613 bacterial strains from a phenanthrene-degrading consortium obtained from a chronically
614 contaminated-soil. Int Biodeterior Biodegradation 85, 42–51.
615 https://doi.org/10.1016/j.ibiod.2013.06.006

616 García-Sánchez, M., Košnář, Z., Mercl, F., Aranda, E., Tlustoš, P., 2018. A comparative study to
617 evaluate natural attenuation, mycoaugmentation, phytoremediation, and microbial-assisted
618 phytoremediation strategies for the bioremediation of an aged PAH-polluted soil. Ecotoxicol
619 Environ Saf 147, 165–174. https://doi.org/10.1016/j.ecoenv.2017.08.012

620 Guo, G., Tian, F., Ding, K., Wang, L., Liu, T., Yang, F., 2017. Effect of a bacterial consortium on the
621 degradation of polycyclic aromatic hydrocarbons and bacterial community composition in
622 Chinese soils. Int Biodeterior Biodegradation 123, 56–62.
623 https://doi.org/10.1016/j.ibiod.2017.04.022

Iwabuchi, N., Sunairi, M., Urai, M., Itoh, C., Anzai, H., Nakajima, M., Harayama, S., 2002. Extracellular polysaccharides of Rhodococcus rhodochrous S-2 stimulate the degradation of aromatic components in crude oil by indigenous marine bacteria. Appl Environ Microbiol 68, 2337–2343. https://doi.org/10.1128/AEM.68.5.2337-2343.2002

Jiang, B., Chen, Y., Xing, Y., Lian, L., Shen, Y., Zhang, B., Zhang, H., Sun, G., Li, J., Wang, X., Zhang, D., 2022. Negative correlations between cultivable and active-yet-uncultivable pyrene degraders explain the postponed bioaugmentation. J Hazard Mater 423. https://doi.org/10.1016/j.jhazmat.2021.127189

Jiménez, D.J., Mares, M.C. De, Salles, J.F., 2018. Temporal expression dynamics of plant biomass-degrading enzymes by a synthetic bacterial consortium growing on sugarcane bagasse. Front Microbiol 9. https://doi.org/10.3389/fmicb.2018.00299

Kaminsky, L.M., Trexler, R. V., Malik, R.J., Hockett, K.L., Bell, T.H., 2019. The Inherent Conflicts in Developing Soil Microbial Inoculants. Trends Biotechnol. https://doi.org/10.1016/j.tibtech.2018.11.011

Kuppusamy, S., Thavamani, P., Venkateswarlu, K., Lee, Y.B., Naidu, R., Megharaj, M., 2017. Remediation approaches for polycyclic aromatic hydrocarbons (PAHs) contaminated soils: Technological constraints, emerging trends and future directions. Chemosphere. https://doi.org/10.1016/j.chemosphere.2016.10.115

Laothamteep, N., Kawano, H., Vejarano, F., Suzuki-Minakuchi, C., Shintani, M., Nojiri, H., Pinyakong, O., 2021. Effects of environmental factors and coexisting substrates on PAH degradation and transcriptomic responses of the defined bacterial consortium OPK. Environmental Pollution 277. https://doi.org/10.1016/j.envpol.2021.116769

Lawson, C.E., 2021. Retooling Microbiome Engineering for a Sustainable Future. mSystems 6. https://doi.org/10.1128/msystems.00925-21

Li, Q., Li, J., Jiang, L., Sun, Y., Luo, C., Zhang, G., 2021. Diversity and structure of phenanthrene degrading bacterial communities associated with fungal bioremediation in petroleum contaminated soil. J Hazard Mater 403. https://doi.org/10.1016/j.jhazmat.2020.123895

Lin, H., Peddada, S. Das, 2020. Analysis of compositions of microbiomes with bias correction. Nat Commun 11. https://doi.org/10.1038/s41467-020-17041-7

Liu, X., Mei, S., Salles, J.F., 2023. Inoculated microbial consortia perform better than single strains in living soil: A meta-analysis. Applied Soil Ecology 190. https://doi.org/10.1016/j.apsoil.2023.105011

Macchi, M., Festa, S., Nieto, E., Irazoqui, J.M., Vega-Vela, N., Junca Howard, Valacco, M.P., Amadio, A.F., Morelli, I.S., Coppotelli, B.M., 2021. Design and evaluation of synthetic bacterial consortia for optimized phenanthrene degradation through the integration of genomics and shotgun proteomics. Biotechnology Reports 29. https://doi.org/10.1016/j.btre.2021.e00588

Mallon, C.A., Le Roux, X., Van Doorn, G.S., Dini-Andreote, F., Poly, F., Salles, J.F., 2018. The impact of failure: Unsuccessful bacterial invasions steer the soil microbial community away from the invader's niche. ISME Journal 12, 728–741. https://doi.org/10.1038/s41396-017-0003-y

Mallon, C.A., Van Elsas, J.D., Salles, J.F., 2015. Microbial invasions: The process, patterns, and mechanisms. Trends Microbiol. https://doi.org/10.1016/j.tim.2015.07.013

Manfredini, A., Malusà, E., Costa, C., Pallottino, F., Mocali, S., Pinzari, F., Canfora, L., 2021. Current Methods, Common Practices, and Perspectives in Tracking and Monitoring Bioinoculants in Soil. Front Microbiol. https://doi.org/10.3389/fmicb.2021.698491

Massot, F., Bernard, N., Alvarez, L.M.M., Martorell, M.M., Mac Cormack, W.P., Ruberto, L.A.M., 2022. Microbial associations for bioremediation. What does “microbial consortia” mean? Appl Microbiol Biotechnol. https://doi.org/10.1007/s00253-022-11864-8

Mawarda, P.C., Le Roux, X., Dirk van Elsas, J., Salles, J.F., 2020. Deliberate introduction of invisible invaders: A critical appraisal of the impact of microbial inoculants on soil microbial communities. Soil Biol Biochem. https://doi.org/10.1016/j.soilbio.2020.107874

McCarty, N.S., Ledesma-Amaro, R., 2019. Synthetic Biology Tools to Engineer Microbial Communities for Biotechnology. Trends Biotechnol. https://doi.org/10.1016/j.tibtech.2018.11.002

Nearing, J.T., Douglas, G.M., Hayes, M.G., MacDonald, J., Desai, D.K., Allward, N., Jones, C.M.A., Wright, R.J., Dhanani, A.S., Comeau, A.M., Langille, M.G.I., 2022. Microbiome differential abundance methods produce different results across 38 datasets. Nat Commun 13. https://doi.org/10.1038/s41467-022-28034-z

Nieto, E.E., Macchi, M., Valacco, M.P., Festa, S., Morelli, I.S., Coppotelli, B.M., 2023. Metaproteomic and gene expression analysis of interspecies interactions in a PAH-degrading synthetic microbial consortium constructed with the key microbes of a natural consortium. Biodegradation. https://doi.org/10.1007/s10532-022-10012-3

Nwankwegu, A.S., Zhang, L., Xie, D., Onwosi, C.O., Muhammad, W.I., Odoh, C.K., Sam, K., Idenyi, J.N., 2022. Bioaugmentation as a green technology for hydrocarbon pollution remediation. Problems and prospects. J Environ Manage. https://doi.org/10.1016/j.jenvman.2021.114313

Pagé, A.P., Yergeau, É., Greer, C.W., 2015. Salix purpurea stimulates the expression of specific bacterial xenobiotic degradation genes in a soil contaminated with hydrocarbons. PLoS One 10. https://doi.org/10.1371/journal.pone.0132062

Palkova, Z., 2004. Multicellular microorganisms: Laboratory versus nature. EMBO Rep. https://doi.org/10.1038/sj.embor.7400145

Pascual-García, A., Bonhoeffer, S., Bell, T., 2020. Metabolically cohesive microbial consortia and ecosystem functioning. Philosophical Transactions of the Royal Society B: Biological Sciences. https://doi.org/10.1098/rstb.2019.0245

Patel, A.B., Shaikh, S., Jain, K.R., Desai, C., Madamwar, D., 2020. Polycyclic Aromatic Hydrocarbons: Sources, Toxicity, and Remediation Approaches. Front Microbiol. https://doi.org/10.3389/fmicb.2020.562813

Pérez-Pantoja, D., Donoso, R., Agulló, L., Córdova, M., Seeger, M., Pieper, D.H., González, B., 2012. Genomic analysis of the potential for aromatic compounds biodegradation in Burkholderiales. Environ Microbiol 14, 1091–1117. https://doi.org/10.1111/j.1462-2920.2011.02613.x

Ravindra, K., Sokhi, R., Van Grieken, R., 2008. Atmospheric polycyclic aromatic hydrocarbons: Source attribution, emission factors and regulation. Atmos Environ. https://doi.org/10.1016/j.atmosenv.2007.12.010

Shi, Y., Delgado-Baquerizo, M., Li, Y., Yang, Y., Zhu, Y.G., Peñuelas, J., Chu, H., 2020. Abundance of kinless hubs within soil microbial networks are associated with high functional potential in agricultural ecosystems. Environ Int 142. https://doi.org/10.1016/j.envint.2020.105869

Silverstein, M.R., Segrè, D., Bhatnagar, J.M., 2023. Environmental microbiome engineering for the mitigation of climate change. Glob Chang Biol. https://doi.org/10.1111/gcb.16609

Steensels, J., Gallone, B., Voordeckers, K., Verstrepen, K.J., 2019. Domestication of Industrial Microbes. Current Biology. https://doi.org/10.1016/j.cub.2019.04.025

Stenuit, B., Agathos, S.N., 2015. Deciphering microbial community robustness through synthetic ecology and molecular systems synecology. Curr Opin Biotechnol. https://doi.org/10.1016/j.copbio.2015.03.012

Tu, Q., Yan, Q., Deng, Y., Michaletz, S.T., Buzzard, V., Weiser, M.D., Waide, R., Ning, D., Wu, L., He, Z., Zhou, J., 2020. Biogeographic patterns of microbial co-occurrence ecological networks in six American forests. Soil Biol Biochem 148. https://doi.org/10.1016/j.soilbio.2020.107897

Wanapaisan, P., Laothamteep, N., Vejarano, F., 2018. Synergistic degradation of pyrene by five culturable bacteria in a mangrove sediment-derived bacterial consortium. J Hazard Mater 342, 561–570. https://doi.org/10.1016/j.jhazmat.2017.08.062

Wang, B., Teng, Y., Xu, Y., Chen, W., Ren, W., Li, Y., Christie, P., Luo, Y., 2018. Effect of mixed soil microbiomes on pyrene removal and the response of the soil microorganisms. Science of the Total Environment 640–641, 9–17. https://doi.org/10.1016/j.scitotenv.2018.05.290

Wilhelm, R.C., Amsili, J.P., Kurtz, K.S.M., van Es, H.M., Buckley, D.H., 2023. Ecological insights into soil health according to the genomic traits and environment-wide associations of bacteria in agricultural soils. ISME Communications 3. https://doi.org/10.1038/s43705-022-00209-1

Willms, I.M., Rudolph, A.Y., Göschel, I., Bolz, S.H., Schneider, D., Penone, C., Poehlein, A., Schöning, I., Nacke, H., 2020. Globally Abundant “Candidatus Udaeobacter” Benefits from Release of Antibiotics in Soil and Potentially Performs Trace Gas Scavenging. https://doi.org/10.1128/mSphere

Willsey, G.G., Wargo, M.J., 2015. Extracellular lipase and protease production from a model drinking water bacterial community is functionally robust to absence of individual members. PLoS One 10. https://doi.org/10.1371/journal.pone.0143617

Yang, Z.N., Liu, Z.S., Wang, K.H., Liang, Z.L., Abdugheni, R., Huang, Y., Wang, R.H., Ma, H.L., Wang, X.K., Yang, M.L., Zhang, B.G., Li, D.F., Jiang, C.Y., Corvini, P.F.X., Liu, S.J., 2022. Soil microbiomes divergently respond to heavy metals and polycyclic aromatic hydrocarbons in contaminated industrial sites. Environmental Science and Ecotechnology 10. https://doi.org/10.1016/j.ese.2022.100169

Zhang, L., Wang, X., Jiao, Y., Chen, X., Zhou, L., Guo, K., Ge, F., Wu, J., 2013. Biodegradation of 4-chloronitrobenzene by biochemical cooperation between Sphingomonas sp. strain CNB3 and Burkholderia sp. strain CAN6 isolated from activated sludge. Chemosphere 91, 1243–1249. https://doi.org/10.1016/j.chemosphere.2013.01.115

Zhang, L., Yi, M., Lu, P., 2022. Effects of pyrene on the structure and metabolic function of soil microbial communities. Environmental Pollution 305, 119301. https://doi.org/10.1016/J.ENVPOL.2022.119301

Zhou, H., Zhang, S., Xie, J., Wei, H., Hu, Z., Wang, H., 2020. Pyrene biodegradation and its potential pathway involving Roseobacter clade bacteria. Int Biodeterior Biodegradation 150. https://doi.org/10.1016/j.ibiod.2020.104961

Zhou, N., Guo, H., Liu, Q., Zhang, Z., Sun, J., Wang, H., 2022. Bioaugmentation of polycyclic aromatic hydrocarbon (PAH)-contaminated soil with the nitrate-reducing bacterium PheN7 under anaerobic condition. J Hazard Mater 439. https://doi.org/10.1016/j.jhazmat.2022.129643

Ziesack, M., Gibson, T., Oliver, J.K.W., Shumaker, A.M., Hsu, B.B., Riglar, D.T., Giessen, T.W., Dibenedetto, N. V, Bry, L., Way, J.C., Silver, P.A., Gerber, G.K., 2019. Engineered Interspecies Amino Acid Cross-Feeding Increases Population Evenness in a Synthetic Bacterial Consortium. mSystems 4, 1–15. https://doi.org/10.1128/msystems.00352-19

7. Figures and Tables

Microcosms	Av degree	Net diam	Av Path Length	Clust coef	Network Density	Nodes	Edges	Positive	Negative
Control d0	31	2	1.261	0.823	0,739	44	699	372	327
Control d15	60	2	1.154	0.914	0,846	73	725	484	241
Control d58	30	2	1.089	0.932	0,911	35	542	261	281
SP+PAH d15	25	2	1.286	0.775	0,714	36	450	250	200
SP+PAH d58	23	2	1.03	0.975	0,975	25	291	140	151
SC AMBk d15	20	2	1.257	0.8	0,743	28	281	162	119
SC AMBk d58	22	2	1.135	0.883	0,865	26	281	177	104
SC1d15	16	2	1.323	0.714	0,677	26	220	150	70
SC1d58	24	2	1.203	0.871	0,832	31	387	171	216
SC4 d15	19	2	1.168	0.826	0,797	26	259	158	101
SC4 d58	24	2	1.043	0.96	0,957	26	311	170	141

Table 1: Network properties of soil bacterial communities in analyzed microcosms.

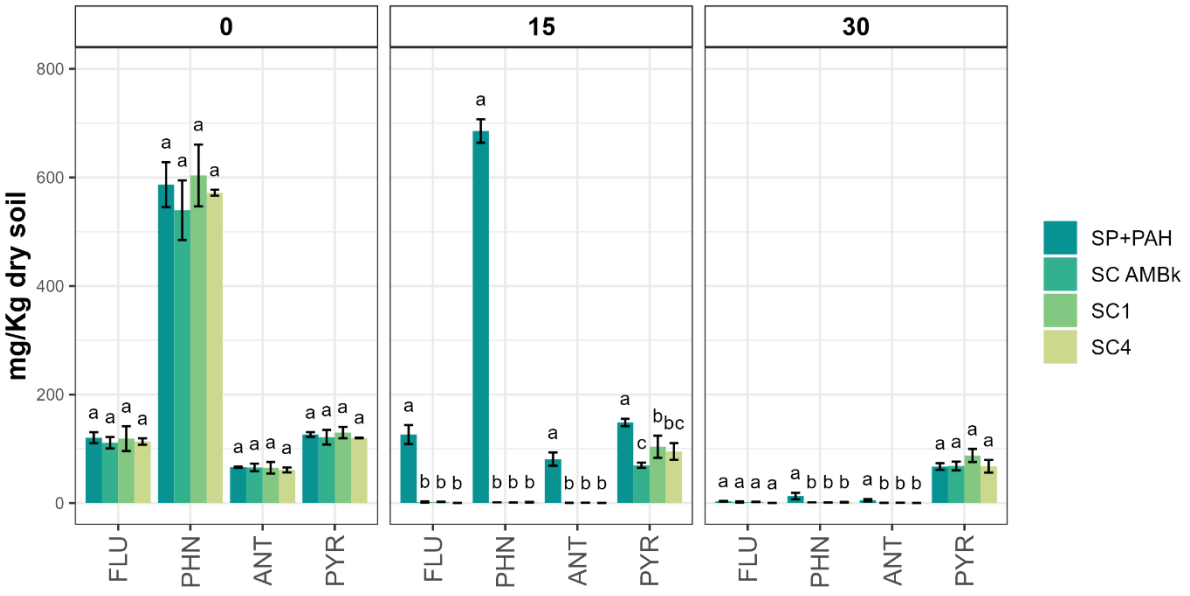

Figure 1: Concentration of supplemented PAHs expressed as mg/Kg of dry soil on day 0 (A) and day 30 (B) of incubation in the inoculated microcosms and in the contaminated control (SP+PAH). The means of independent triplicates with their respective standard deviations are shown. Fluorene (FLU), phenanthrene (PHN), anthracene (ANT) and pyrene (PYR). The non-contaminated control (control) and day 58 of all treatments were excluded from figure, as the concentration of PAHs was below the detection limit.

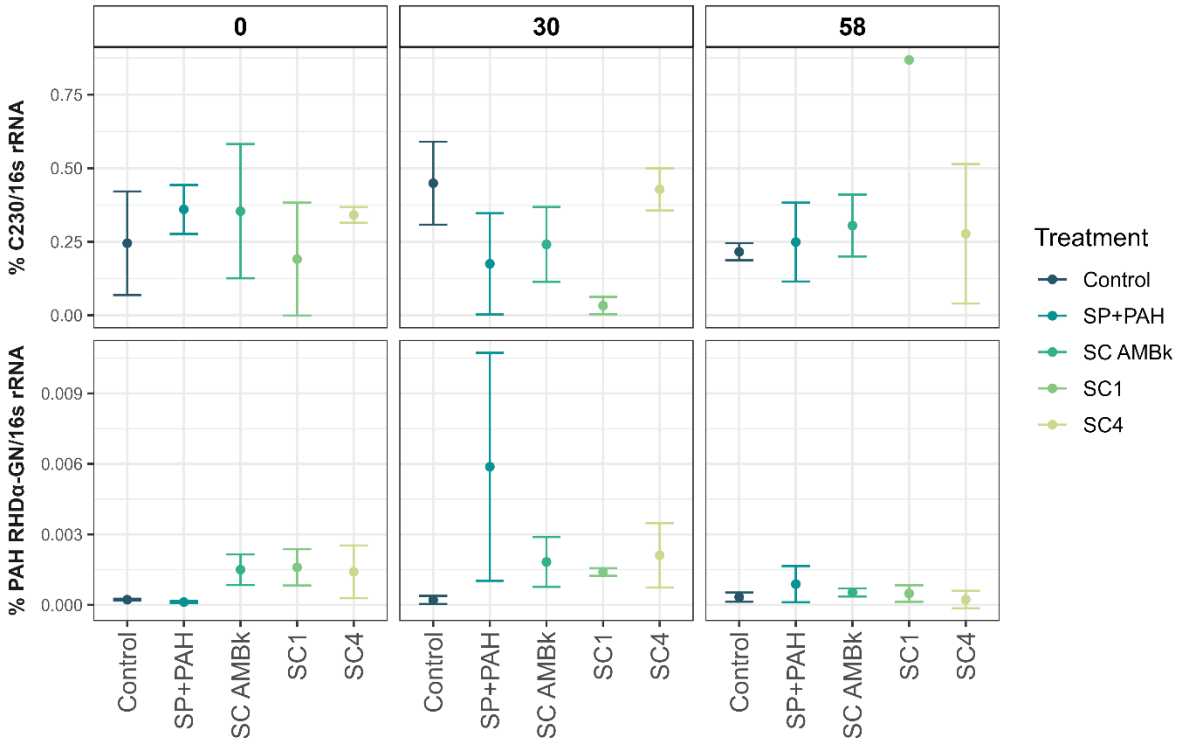

768

769 Figure 2: Percentage ratio between the number of copies of the specific gene (C230 gene or PAH RDHα-

770 GN gene) and the number of copies of the 16S rRNA gene for the inoculated microcosms and the

771 controls. The means of triplicate are plotted with their respective standard deviations.

772

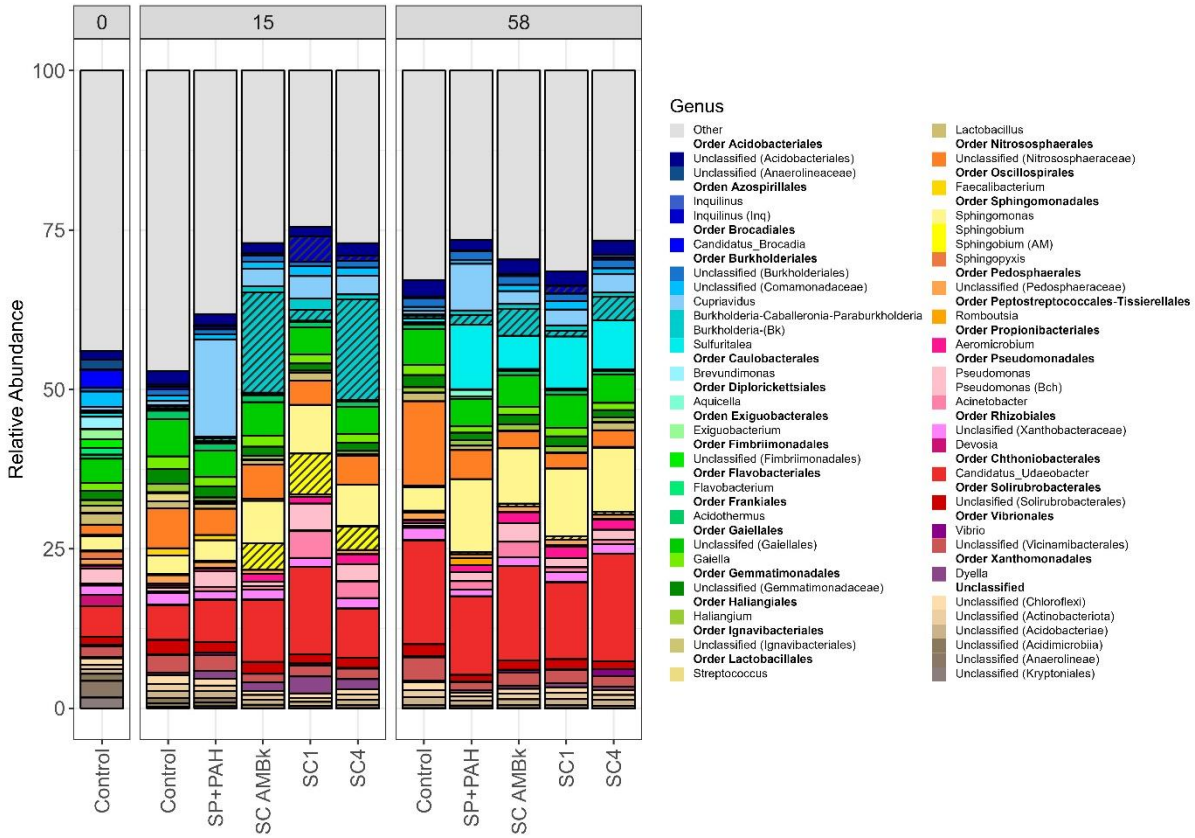

Figure 3. Relative abundances of the genera whose abundance exceeds 1% in the microcosms analyzed at 15 and 58 days of incubation. These genera represented more than 50% of the relative abundance of the community. The average of the triplicates for each treatment is shown. The dashed plot identifies the contribution of ASVs identified with each of the strains to the corresponding genus.

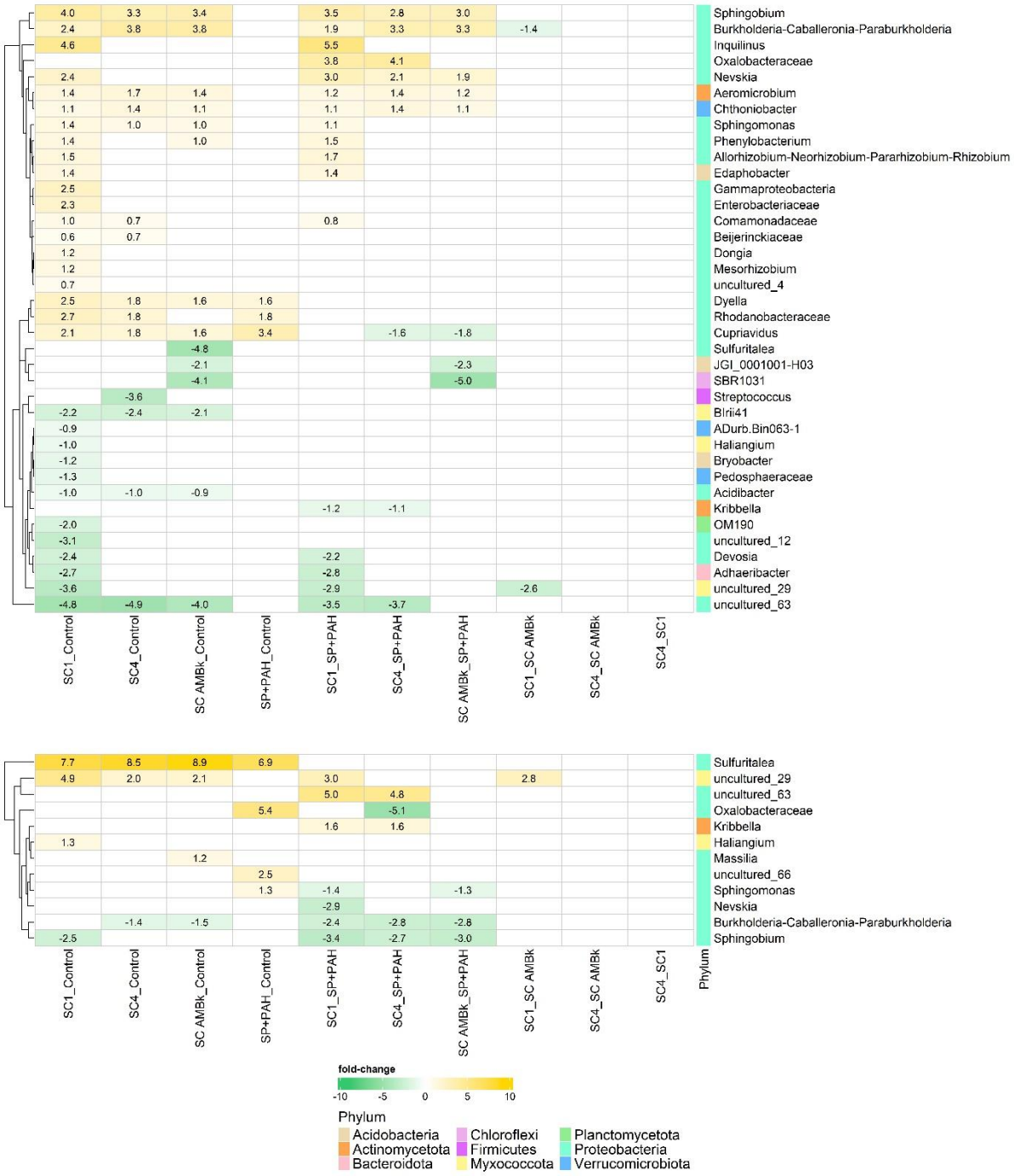

Figure 4: Microbiome genera for which significant changes in absolute abundances were observed between the microcosms analyzed at 15 and 58 days of incubation. Results were expressed as the log fold-change (lfc) of the comparisons between treatments.

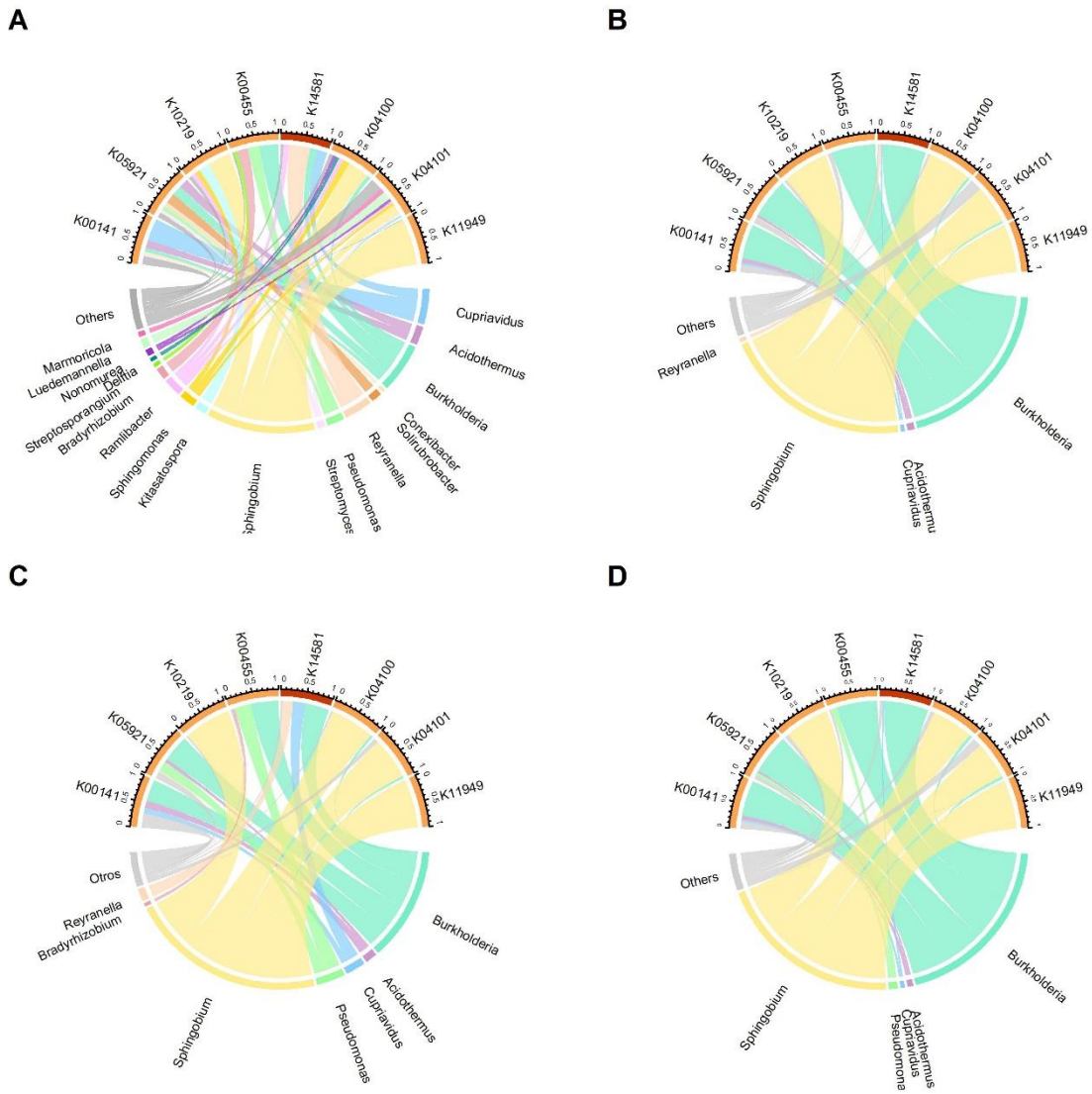

Figure 5: Chord diagram showing the relative contribution for 5 KOs predicted by PICRUSt2, which showed significant differences in SP+PAH contaminated microcosms (A), inoculated with SC AMBk (B), SC1 (C) and SC4 (D) at 15 days of incubation. The averages of the relative contributions are shown for the genera whose relative contributions were greater than 5% in at least one route. Those KOs related to the lower PAH degradation pathway are shown in orange while the KO linked to the high degradation pathway is shown in red.

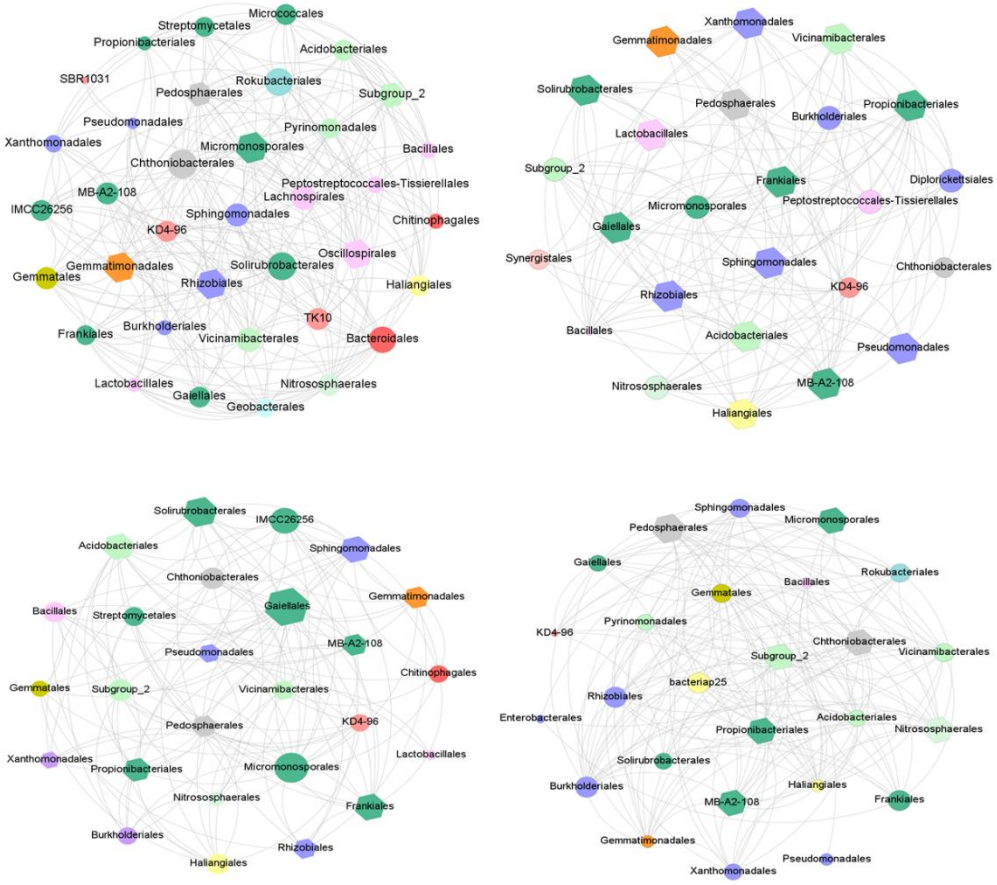

Figure 6: Network co-occurrence analysis of the microbiomes in SP+PAH (A) and inoculated (B) microcosms at day 15 of incubation. A connection stands for a strong (SparCC r > 0.5) and positive correlation (p value < 0.05). The size of each node is proportional to the number of connections (degree). Each node is colored based on the bacterial phyla and keystone taxa are indicated as hexagons.